Investigation of process parameters for stable micro dry wire electrical discharge machining

The International Journal of Advanced Manufacturing Technology

July 2019, Volume 103, Issue 1–4, pp 723–741 | Cite as

- Asfana Banu (1)
- Mohammad Yeakub Ali (1) Email author (mmyali@iium.edu.my)
- Mohamed Abdul Rahman (1)
- Mohamed Konneh (1)

1. Department of Manufacturing and Materials Engineering, Faculty of Engineering, International Islamic University Malaysia, , Kuala Lumpur, Malaysia

ORIGINAL ARTICLE
First Online: 25 March 2019

Abstract

Micro dry wire electrical discharge machining (μDWEDM) is a process where gas is used as the dielectric fluid instead of a liquid. In this process, certain modifications of wire electrical discharge machining (WEDM) are needed during the machining operation to achieve stable machining. Smooth and stable machining operation in μDWEDM process remains as a critical issue. Thus, this paper presents the investigation of process parameters for a stable μDWEDM process. The investigation was performed on a stainless steel (SS304) with a tungsten wire as the electrode using integrated multi-process machine tool, DT 110 (Mikrotools Inc., Singapore). The experimentation method used in this phase was a conventional experimental method, one-factor-at-a-time

Investigation of process parameters for stable micro dry wire electrical discharge machining

Asfana Banu, Mohammad Yeakub Ali, Mohamed Abdul Rahman & Mohamed Konneh

The International Journal of Advanced Manufacturing Technology

ISSN 0268-3768
Volume 103
Combined 1-4

Int J Adv Manuf Technol (2019)
103:723-741
DOI 10.1007/s00170-019-03603-7

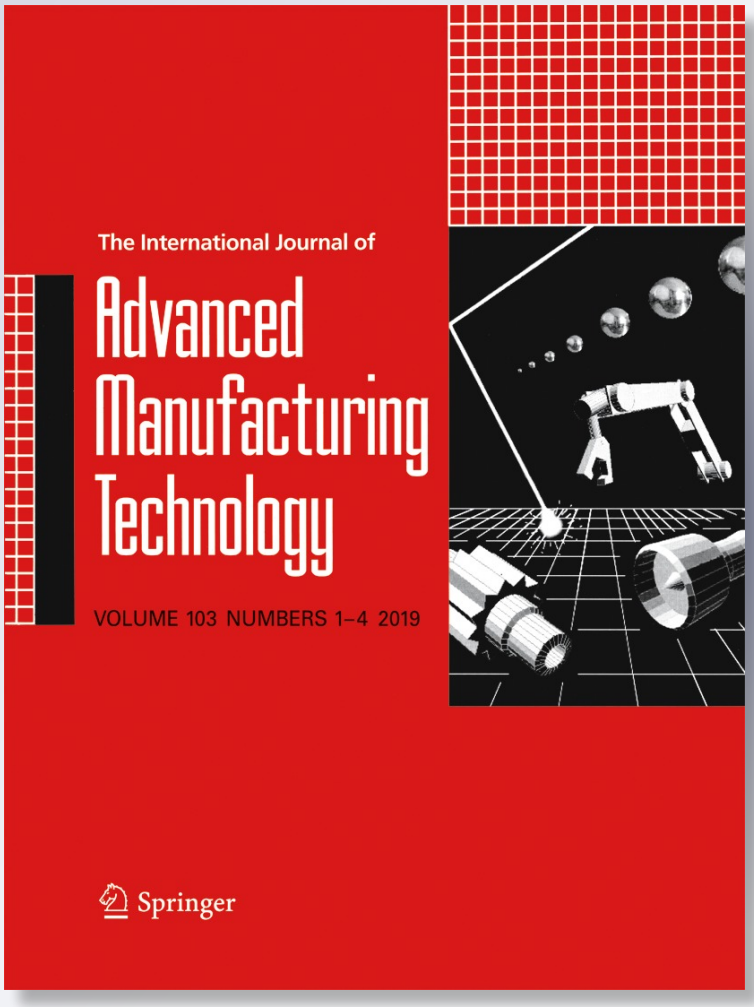

Springer

The International Journal of Advanced Manufacturing Technology (2019) 103:723–741
https://doi.org/10.1007/s00170-019-03603-7

ORIGINAL ARTICLE

Investigation of process parameters for stable micro dry wire electrical discharge machining

Asfana Banu[1] · Mohammad Yeakub Ali[1] · Mohamed Abdul Rahman[1] · Mohamed Konneh[1]

Received: 13 December 2018 / Accepted: 13 March 2019 / Published online: 25 March 2019

Abstract

Micro dry wire electrical discharge machining (μDWEDM) is a process where gas is used as the dielectric fluid instead of a liquid. In this process, certain modifications of wire electrical discharge machining (WEDM) are needed during the machining operation to achieve stable machining. Smooth and stable machining operation in μDWEDM process remains as a critical issue. Thus, this paper presents the investigation of process parameters for a stable μDWEDM process. The investigation was performed on a stainless steel (SS304) with a tungsten wire as the electrode using integrated multi-process machine tool, DT 110 (Mikrotools Inc., Singapore). The experimentation method used in this phase was a conventional experimental method, one-factor-at-a-time (OFAT). Types of dielectric fluid, dielectric fluid pressure, polarity, threshold, wire tension, wire feed rate, wire speed, gap voltage, and capacitance were the controlled parameters. The machined microchannels were observed using scanning electron microscope (SEM). Stable and smooth machining operation of μDWEDM was found to be with compressed air as the dielectric fluid, workpiece positive polarity, 24% threshold, 0.0809 N wire tension, 0.2 μm/s wire feed rate, and 0.6 rpm wire speed.

Keywords Dry EDM · DEDM · Dry WEDM · DWEDM · Micro dry wire EDM · μDWEDM

1 Introduction

The increasing demands for miniaturized products especially in the biomedical, electronics, and aerospace industry have obliged the manufacturers to fabricate complex micro parts with high accuracy and nano surface finish. Micro wire electrical discharge machining (μWEDM) is one of the flexible machining processes that are capable in producing complex three-dimensional (3D) miniaturized parts [35, 36, 70]. It is thermal machining where the material from the workpiece is removed by the thermal energy created by the electrical spark [36, 73, 74]. A series of electrical sparks or discharges occur rapidly in a short span of time within a constant spark gap between the micro sized tool electrode and the workpiece material. In this process, the tool and the workpiece both are adequately immersed in a dielectric fluid [15, 16, 36]. Dielectric fluid plays an important role in μWEDM process as a coolant and also helps to flush away the debris from the machining gap. In addition, the dielectric fluid also helps to improve the efficiency of the machining operation as well as improving the quality of the machined parts. Commonly used dielectric fluids are mineral oil-based liquid or hydrocarbon oils which have the tendency to cause fire hazard and environmental problems such as the production of very toxic and non-recyclable dielectric wastes and fumes that may cause health hazard to the users [10, 13, 20, 48, 68, 75, 100].

In order to overcome these problems, researchers have introduced dry wire electrical discharge machining (DWEDM) and micro dry wire electrical discharge machining (μDWEDM) [10, 35, 36, 94]. DWEDM is a modified wire electrical discharge machining (WEDM) process where gas dielectric is used instead of liquid dielectric fluid. The high-pressured flow of gas helps to remove the debris and also avoids unnecessary heating of the wire and the workpiece at the discharge gap. Near-zero tool wear, better surface quality, lower residual stresses, thinner white layer, and higher precision and accuracy are the prime attraction of this dry technique [1, 10, 49, 53, 88, 93]. It is highly recommended to use dry EDM (DEDM) for finish cut with high-surface quality (0.04–

✉ Mohammad Yeakub Ali
mmyali@iium.edu.my

[1] Department of Manufacturing and Materials Engineering, Faculty of Engineering, International Islamic University Malaysia, P.O. Box 10, 50728 Kuala Lumpur, Malaysia

0.25 μRa) especially in machining high-precision dies and molds [1, 27, 34]. This concept also needs to apply in micro dry EDM (μDEDM) where the process has not yet been established. Compared to conventional WEDM, lower wire electrode vibration, narrower gap distance, and negligible process reaction enable μDWEDM to achieve high accuracy of the finishing cut [93, 99]. The commonly used gas dielectric fluids are atmospheric air, compressed air, liquid nitrogen, oxygen, argon, and helium [14, 71, 88].

However, without fundamental understanding of the machining mechanism, a stable and smooth machining using μDWEDM is unattainable due to process interruption such as wire breakage, poor machining stability and arcing, and inefficiency in debris expulsion [32, 75, 93]. Hence, in the present state of the arts, stable and smooth machining process using μDWEDM remains as a critical issue. Therefore, the main objective of this research is to investigate μDWEDM process to identify the influential process parameters for stable and smooth machining process.

2 Methodology

The investigation of μDWEDM process was performed on a stainless steel (SS304) plate (30 mm × 20 mm × 0.5 mm) with tungsten (W) wire of 70 μm in diameter as the electrode. Stainless steel is usually used in most of the industrial application including manufacturing miniaturize products such as micro-fins for cooling purposes for electronic components [60, 66, 103]. Stainless steel becomes the most preferred material for industrial application due to its high hardenability as well as resistance against corrosion and chemical [3]. Tungsten wire with small radii (0.025–0.1 mm) is preferable since it has high tensile strength (> 1900 MPa), resistance to erosion, and load-carrying capability. Besides that, the accuracy of the machined slot and the precision of the process improve when tungsten wire is used as the electrode. Moreover, this wire is suitable in producing small features with very high tolerances and good surface finish [28, 39, 58, 76]. The properties of these two materials are listed in Tables 1 and 2.

Before starting the experiment, the workpiece was grounded manually using 320, 400, 600, and 800 grades of sand papers, respectively. Then, the workpiece was immersed in ethanol and cleaned for 5 min by ultrasonic cleaning machine (BRANSON 2510, Virginia). Ultrasonic cleaning is useful in removing the micro size dirt particles. After preparing the sample, μDWEDM process was conducted on the workpiece using the integrated multi-process machine tool DT-110 (Mikrotools Inc., Singapore). The machine has a real-time sensor where it controls the tension and motion in order to maintain a sufficient gap distance between the workpiece and the tool electrode [2, 18]. When the machining was completed, the workpiece once again was immersed in ethanol and cleaned for 5 min using ultrasonic cleaning machine. The machined surface was then inspected using scanning electron microscope (SEM) (JEOL JSM-5600, Japan). SEM is a basic type of electron microscope, where it is capable in producing high-resolution three-dimensional images in order to study the microstructure morphology of a specimen [31, 92, 102].

Several types of parameters were involved to achieve a stable and smooth μDWEDM operation. This is because whenever the machining operation was conducted, the wire would break easily. That is why the parameters were not only selected based on the literature review but also based on the capability of the machine, type of machining material, and tool electrode [8]. The parameters involved during the experimental investigation were types of dielectric fluid, dielectric fluid pressure, polarity, threshold, wire tension, wire feed rate,

Table 2 Properties of the tungsten wire electrode (Ø 70 μm)

Properties	Tungsten (W)
Thermal expansion (μm/m/K)	4.5
Thermal conductivity (W/m/K)	173
Tensile strength (MPa)	> 1900
Electrical resistivity (nΩ/m)	52.8
Young's modulus (GPa)	411
Shear modulus (GPa)	161
Bulk modulus (GPa)	310
Poisson ratio	0.28
Mohs hardness	7.5
Vickers hardness (MPa)	3430–4600
Brinell hardness (MPa)	2000–4000

From Puri [76] and Maher et al. [58]

Table 1 Properties of the stainless steel (SS304) [12]

Chemical composition (%)							
C	S	P	Mn	Si	Cr	Ni	N
0.030	0.030	0.045	2.00	0.75	17.5–19.5	8.0–10.5	0.1
Mechanical properties							
Tensile strength, Rm (MPa)	Yield stress, $Rp_{0.2\%}$ (MPa)	Elongation, A_5 (%)	Rockwell hardness (HRBW)		Heat treatment		
					Anneal (°C)	Quench	
515	205	40	92		1050–1100	Air/spray	

wire speed, gap voltage, and capacitance. The experimentation approach used for this phase was one-factor-at-a-time (OFAT). The experiments for each of the factors were repeated three times which means that three different microchannels were machined for each of the experiments. The average of the machining length from these three microchannels as well as their standard deviations was calculated, and the results are presented in Sect. 3. The experimental results were scrutinized with analysis of standard deviation and statistical test using Levene's test. The Levene's test [26, 62] results were found insignificant in few cases. However, we still continue this experimental investigation based on standard deviation (Tables 4, 5, 6, 7, 8, 9, 10, 11, and 12), as this is the first investigation without having any previous results. The controlled and fixed parameters are listed in Table 3.

3 Results and discussions

In this section, the results are discussed in detail. The results of the experiments are based on the SEM images of the microchannels and the scatter graphs. The machining length in the scatter graphs determines the materials removed from the workpiece.

3.1 Dielectric fluid

Dielectric fluid is important in initiating the electrical discharge between the wire electrode and the workpiece, improves the efficiency of the machining process, improves quality of the machined parts, and flushes away the debris from the machining gap [10, 13, 20, 48, 68, 75, 100]. Figure 1a, b shows the machining setup with atmospheric air and compressed air as the dielectric fluid, respectively, while Fig. 1c, d shows the close-up position of the workpiece when atmospheric air and compressed air are used as the dielectric fluid, respectively. The compressed air supplies dry air without any moisture [30]. However, in this investigation, the position of the nozzle and the direction of the compressed air were kept fixed (10 mm away from workpiece at ≈ 60° angle with the wire axis) (Fig. 1d). These dielectric fluids were selected based on their ability to machine finishing cut features with high accuracy and precision [1, 24, 48].

Figure 2 shows the illustration of the machining outcome during the machining process, while Fig. 3 shows the results of the machining outcome based on the SEM images of the microchannels with constant parameters 90 V gap voltage, workpiece positive polarity, 0.10 nF capacitance, 0.2 μm/s wire feed rate, 24% threshold, 0.0809 N wire tension, and 0.5 rpm wire speed. Based on the schematic diagram shown in Fig. 2a, minor machining was possible when atmospheric air was used as the dielectric fluid. It is proven by the SEM image shown in Fig. 3a. Wire breakage tends to occur when the machining operation continues. It is most probably happens due to the unwanted debris at the machining area which may cause short circuit that leads to poor surface finish [5–7] and wire breakage. Besides that, when the electrical discharges are concentrated at a certain point with high temperature due to the wire material yielding and fracture, the possibility for the wire to break is high [34, 40, 68].

As for Fig. 2b, the schematic diagram shows a smooth machining operation when the compressed air is used as the

Table 3 Micro dry wire EDM machining conditions for process parameter selection

Controlled parameters	Experimental conditions
Dielectric fluid	1. Atmospheric air
	2. Compressed air
Dielectric fluid pressure for compressed air (MPa)	1. 0.0345 (5 psi)
	2. 0.0689 (10 psi)
	3. 0.1034 (15 psi)
Polarity	1. Workpiece positive
	2. Workpiece negative
Threshold (%)	25, 24, 23
Wire tension (N)	0.0809, 0.1214
Wire feed rate (μm/s)	0.2, 0.4
Wire speed (rpm)	0.5, 0.6
Capacitance (nF)	100, 10, 1.00, 0.10, 0.01
Gap voltage (V)	80, 90, 100, 110
Fixed parameters	
Workpiece	Stainless steel (SS304) (500 μm thickness)
Electrode	Tungsten wire (Ø 70 μm)
Machining length (μm)	300

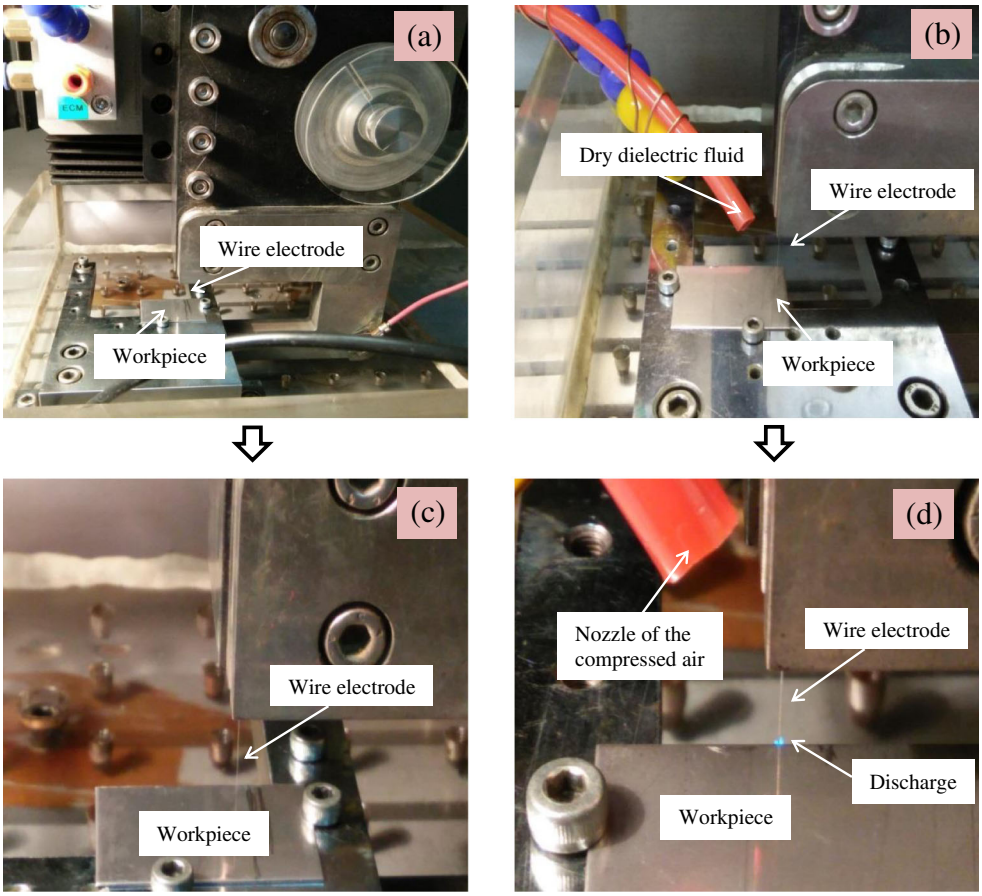

Fig. 1 Machining setup with (**a**) atmospheric air and (**b**) compressed air as the dielectric fluid. Close-up workpiece position when (**c**) atmospheric air and (**d**) compressed air are used as the dielectric fluid

dielectric fluid which is supported by the SEM image of the microchannel in Fig. 3b. The machining was stable and smooth when the air from the compressed air was supplied continuously at the machining area. Moreover, the unwanted debris was flushed away from the machining gap during the machining operation. Besides that, excessive heating between the workpiece and the wire electrode at the machining gap was avoided [10, 27, 49, 53, 88, 93] since the wire was intact.

The experimental results of the machining length with standard deviation for two different types of dielectric fluids are tabulated in Table 4, while Fig. 4 shows the scatter graph of the machining length with respect to gap voltage for combination of dielectric fluid and dielectric fluid pressure. When the machining operation continues further than the machining length tabulated in Table 4, wire breakage would take place and the machining operation would stop. Based on the table and the graph, it is confirmed that the compressed air gives better outcome where the machining length are around 170 to 300 μm. On the other hand, the machining length when the atmospheric air is used as the dielectric fluid is less than

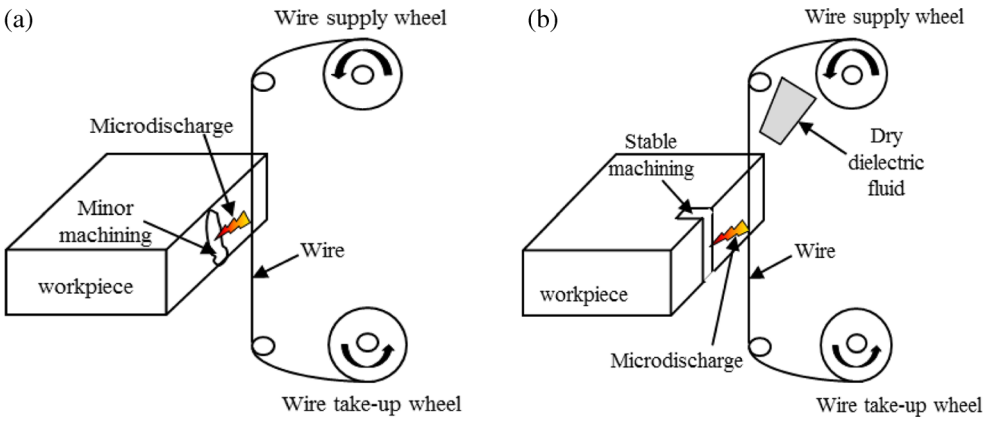

Fig. 2 Schematic diagram of machining outcome during the machining process when (**a**) atmospheric air and (**b**) compressed air are used as the dielectric fluid

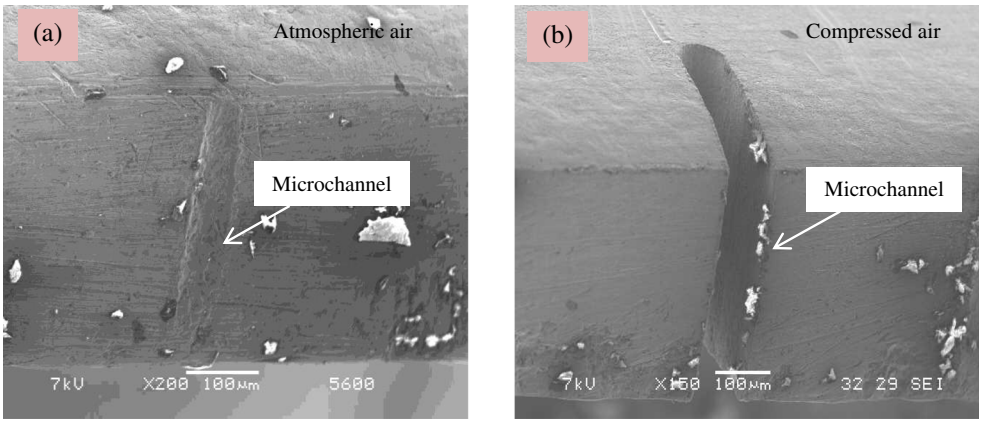

Fig. 3 SEM images for machined area on stainless steel machined with μDWEDM. Parameters: 90 V gap voltage, workpiece positive polarity, 0.10 nF capacitance, 0.2 μm/s wire feed rate, 24% threshold, 0.0809 N wire tension, 0.5 rpm wire speed, and (**a**) atmospheric air and (**b**) compressed air with 0.0345 MPa as dielectric fluid

65 μm. The main reason behind this circumstance is due to the phenomenon of breakdown voltage in gas as stated by the modified Paschen's law.

According to the modified Paschen's law, the breakdown voltage (micro-breakdown) phenomenon solely dependent on the gap distance between the electrodes, *d* rather than the gas pressure and the gap distance between the electrodes (*pd*) as mentioned by the classical Paschen's law [21, 29, 43, 50, 54, 77, 95]. However, in this case, the gas pressure is necessary because the air flow from the compressed air with 0.0345 MPa pressure helps to maintain the ideal gap distance between the electrodes (workpiece and wire electrode) which allows the breakdown voltage to take place in order to form the microplasma. Therefore, compressed air as dielectric fluid would be the best choice since it provides a continuous air flow with 0.0345 MPa pressure at the machining area compared to the atmospheric air.

3.2 Dielectric fluid pressure

When gas is used as the dielectric fluid in μDWEDM, it is necessary to determine its pressure during the machining operation. It is crucial since it affects the formation of microplasma which is determined through the micro-breakdown mechanism during the machining operation [54, 56, 77]. The dielectric fluid pressure for this machining operation was controlled using the air pressure regulator. Figures 5 and 6 show the SEM images for three different dielectric fluid pressures: 0.0345 MPa, 0.0689 MPa, and 0.1034 MPa; with constant parameters 90 V gap voltage, compressed air as the dielectric fluid, 1 nF capacitance, 0.2 μm/s wire feed rate, 24% threshold, 0.0809 N wire tension, workpiece positive polarity, and 0.5 rpm wire speed. Based on these figures, when the dielectric fluid pressure is more than 0.0345 MPa, the microchannels produced have shorter machining length (Figs. 5b and 6) since the wire tends to break in the midst of the machining operation. Even though dielectric fluid pressure affects the kerf of the machined slot in DWEDM [42], but in μDWEDM, the dielectric fluid pressure affects the process stability where the wire breaks during the machining operation.

Besides that, Fig. 6 shows that the workpiece melted in one direction (left side of the SEM images) beyond the machining area of the microchannel. This situation is due to the arcing phenomenon during the machining operation. Arcing is considered as a harmful discharge that leads to an unstable

Table 4 Experimental results for average machining length and standard deviation with two different types of dielectric fluids

Dielectric fluid	Gap voltage (V)	Machining length (μm)			Average machining length (μm)	Standard deviation
		Trial 1	Trial 2	Trial 3		
Atmospheric air (0 MPa)	80.00	64.80	35.30	40.00	46.70	15.85
	90.00	56.90	64.80	30.50	50.73	17.96
	100.00	51.50	41.80	15.70	36.33	18.52
	110.00	36.00	0.00	17.40	17.80	18.00
Compressed air (0.0345 MPa)	80.00	180.00	166.40	170.90	172.43	6.93
	90.00	300.00	286.40	295.60	294.00	6.94
	100.00	277.80	265.70	285.90	276.47	10.17
	110.00	181.60	197.80	205.70	195.03	12.29

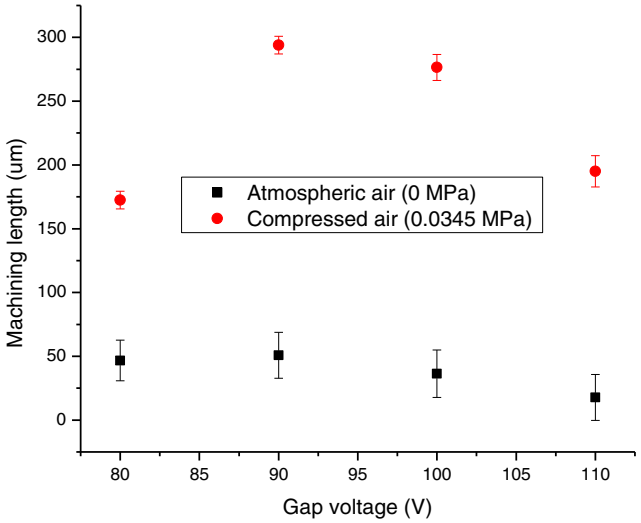

Fig. 4 Graph of machining length with respect to gap voltage for combination of dielectric fluid and dielectric fluid pressure as indicated by the legend. Compressed air (0.0345 MPa) gives higher machining length compared to the atmospheric air (0 MPa) with respect to gap voltage. Based on the results, it shows that the machining is more sustainable when higher dielectric fluid pressure is used. Looking at these, dielectric fluid pressure has more significant role compared to the dielectric fluid. Therefore, detailed investigation on dielectric fluid pressure is discussed in Sect. 3.2. In the experimental results, it was found that 90–100 V gap voltage has the highest level of sustainability. Fixed parameters: 1 nF capacitance, 24% threshold, workpiece positive polarity, 0.2 μm/s wire feed rate, 0.0809 N wire tension, and 0.5 rpm wire speed

machining operation, excessive electrode wear (wire stuck and break), thermal damage (melting) on the workpiece and the electrode surface, and also damages the power supply of the machine [19, 67, 81, 98]. It usually happens when there is excessive discharge energy in the inter-electrode gap generated within the dielectric. Incorrect process parameters and improper flushing condition are the reasons that cause the arcing phenomenon [19, 67].

Table 5 shows the experimental results of the machining length together with the standard deviation for three different dielectric fluid pressures: 0.0345 MPa, 0.0689 MPa, and 0.1034 MPa. Meanwhile, Fig. 7 shows the scatter graph of the machining length with respect to gap voltage for dielectric fluid pressure. For dielectric fluid pressure 0.0689 MPa and 0.1034 MPa, the machining operation was very unstable since the wire easily breaks if the machining operation continues further than the machining length tabulated in Table 5. Moreover, the surface of the workpiece is also damaged quite severely as shown in Fig. 6. Hence, based on Table 5 and Fig. 7, it is verified that 0.0345 MPa dielectric fluid pressure gives better outcome with stable machining process since the machining length of the microchannels is longer (≈ 231–300 μm) and with wire was unharmed. This situation can be explained by the modified Paschen's law as mentioned in Sect. 3.1, where it is stated that the micro-breakdown mechanism is actually influenced by the gap distance between the electrodes (d) rather than the pressure of the gas and the gap distance between the electrodes (pd) [21, 29, 43, 50, 54, 77, 95].

When modified Paschen's law is applied in micro-breakdown mechanism, then ion-enhanced field emission plays a significant role in generating the microplasma [50]. This is because the ion-enhanced field emission actually acts as an additional electron source to the microplasma through the new field emission-driven microdischarges also known as the field emission-driven Townsend discharges. It is a theory where massive amount of electrons are supplied from the field emission instead of ionization or secondary emission [29, 51, 78, 83, 84, 90]. In addition, the main cause for the deviation of the Paschen's law is in fact related to the electric field, E, where it influences the electron emission as expressed by the Eq. 1 [29, 44, 45, 51, 54–56, 78].

$$\gamma_{eff} = Ke^{-D/E} \tag{1}$$

where K and D = constants that depend on material and gas, while E = electric field near the cathode. Constant K is determined based on the ratio of the field emission current density to the positive ion current density onto the cathode [78].

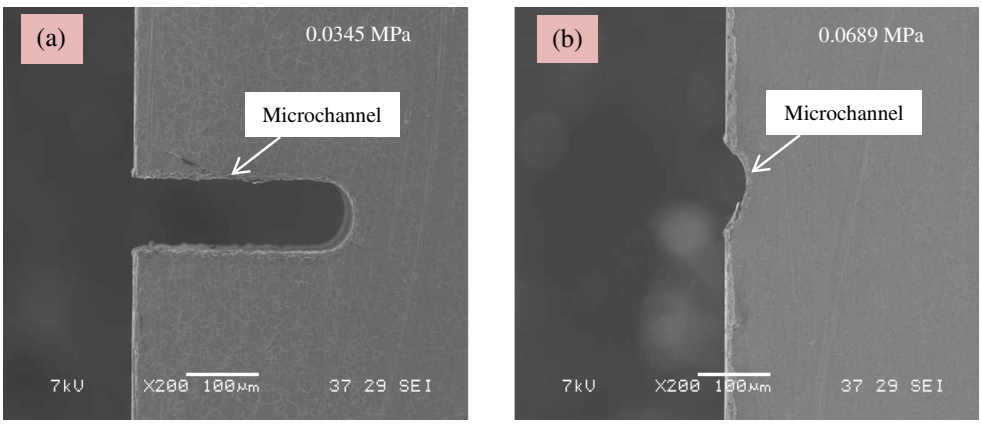

Fig. 5 SEM images for machined area of stainless steel machined with μDWEDM. Parameters: 90 V gap voltage, compressed air as dielectric fluid, 1 nF capacitance, 0.2 μm/s wire feed rate, 24% threshold, 0.0809 N wire tension, workpiece positive polarity, 0.5 rpm wire speed, and (**a**) 0.0345 MPa and (**b**) 0.0689 MPa dielectric fluid pressure

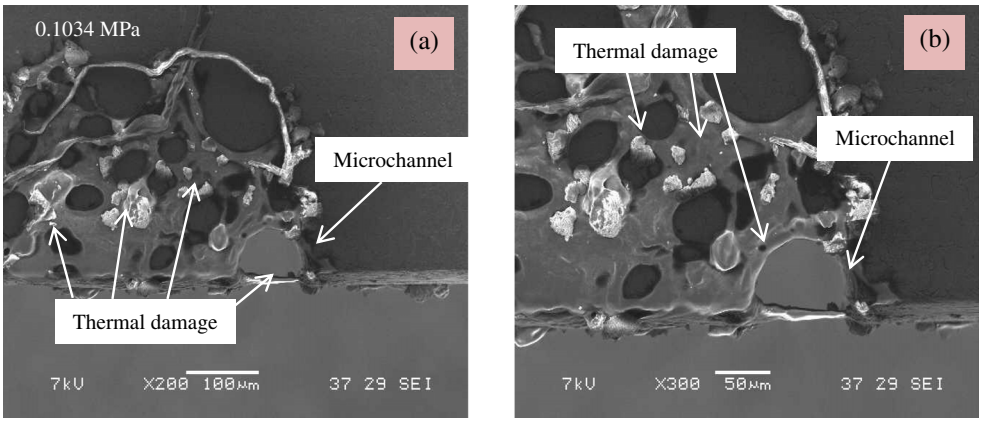

Fig. 6 SEM images with (**a**) × 200 magnification and (**b**) × 300 magnification for machined area of stainless steel machined with μDWEDM. Parameters: 90 V gap voltage, compressed air as dielectric fluid, 1 nF capacitance, 0.2 μm/s wire feed rate, 24% threshold, 0.0809 N wire tension, workpiece positive polarity, 0.5 rpm wire speed, and 0.1034 MPa dielectric fluid pressure

As concluded in the previous section, even though the dielectric fluid pressure is necessary during the machining operation in maintaining the gap distance between the electrodes, but, the ideal dielectric fluid pressure for the compressed air in μDWEDM is 0.0345 MPa rather than the 0.0689 MPa and 0.1034 MPa since higher pressure damages the electrode and the workpiece surfaces.

3.3 Workpiece polarity

Polarity is an important parameter where it has significant implications on speed, stability of the machining operation, material removal rate, electrode wear ratio, and surface roughness [64, 80]. Moreover, with a complete circuit, discharges are formed when the current passes through the machining gap causing the electrode materials to melt and evaporate [41, 87]. Thus, Fig. 8 shows the SEM images of the machined area for two different types of polarity variations with constant parameters 90 V gap voltage, atmospheric air as dielectric fluid, 10 nF capacitance, 0.4 μm/s wire feed rate, 24% threshold, 0.809 N wire tension, and 0.5 rpm wire speed. The variations of the polarity for the electrodes were as follows:

1. Workpiece positive (anode), wire electrode negative (cathode) (Fig. 8a)
2. Workpiece negative (cathode), wire electrode positive (anode) (Fig. 8b)

Based on the SEM images, it is observed that huge amount of material is removed when the workpiece polarity is positive (Fig. 8a) compared to the amount of material removed when the workpiece polarity is negative (Fig. 8b). Furthermore, in Fig. 8b, it is also observed that only a small crater is formed on the workpiece. It is because the wire would break and the machining operation halts once there is a discharge occurred between the workpiece and the wire at the inter-electrode gap. Since the wire tends to break easily with only a discharge, then, it shows that the wire wear is high [27]. Hence, the

Table 5 Experimental results for average machining length and standard deviation with three different dielectric fluid pressures

Dielectric fluid pressure (MPa)	Gap voltage (V)	Machining length (μm)			Average machining length (μm)	Standard deviation
		Trial 1	Trial 2	Trial 3		
0.0345	80.00	300.00	295.70	289.20	294.97	5.44
	90.00	300.00	300.00	283.50	294.50	9.53
	100.00	293.80	284.40	277.60	285.27	8.13
	110.00	247.80	231.80	253.90	244.50	11.41
0.0689	80.00	116.00	97.10	84.30	99.13	15.95
	90.00	72.30	96.80	73.00	80.70	13.95
	100.00	66.30	65.30	73.50	68.37	4.47
	110.00	95.30	92.00	107.00	98.10	7.88
0.1034	80.00	103.00	94.80	84.50	94.10	9.27
	90.00	97.80	91.80	111.00	100.20	9.82
	100.00	62.50	70.50	82.50	71.83	10.07
	110.00	47.50	41.80	37.80	42.37	4.87

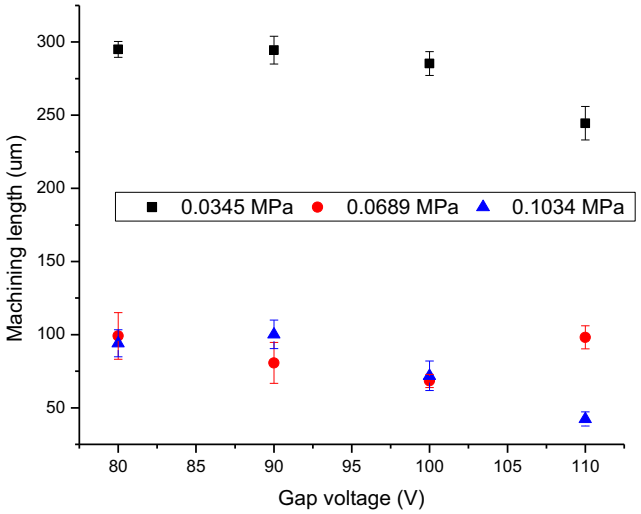

Fig. 7 Graph of machining length with respect to gap voltage for dielectric fluid pressure as indicated by the legend. Dielectric fluid pressure, 0.0345 MPa, the highest machining length followed by 0.0689 MPa and 0.1034 MPa with respect to gap voltage. Looking at this, low dielectric pressure gives more sustainable machining. Hence, it proves that the dielectric fluid pressure does have a significant role during the machining process when it is compared to Fig. 4. It was also found that the highest level of sustainability is between 80 and 100 V gap voltage. Fixed parameters: 10 nF capacitance, 24% threshold, compressed air as dielectric fluid, workpiece positive polarity, 0.2 μm/s wire feed rate, 0.0809 N wire tension, and 0.5 rpm wire speed

occurrence of this phenomenon is due to the formation of the hot anode vacuum arcs (HAVA) [54, 56, 61, 77].

As per discussed in Sect. 3.2, even though modified Paschen's law plays an important role in micro-breakdown mechanism, but the mechanism is actually similar to the vacuum breakdown [54, 55, 78] when the gap distance between the electrodes is less than 5 μm [82, 95]. The phenomenon is caused by the electrons from the field emission [54, 55, 78]. Therefore, this circumstance leads to the generation of microplasma which is enhanced by the ion-enhanced field emission [50]. This brief explanation justifies the formation of the DEDM microplasmas that leads to the formation of a specific type of vacuum discharge known as HAVA [54, 56, 57, 61, 77, 95].

Table 6 shows the experimental results for the average machining length and standard deviation with different workpiece polarity, while Fig. 9 shows the scatter graph of machining length with respect to gap voltage for several combinations of dielectric fluid pressure and workpiece polarity. Based on the table and the graph, it is observed that the most stable machining operation with undamaged wire is when the workpiece polarity is positive with compressed air as the dielectric fluid. The machining lengths of the microchannels are approximately 166 to 300 μm. It occurs due to the HAVA since it causes large amount of anode (workpiece positive) material erosion. The occurrence of the erosion is because of the concentrated discharges dominated by the vacuum arcs at the hot anode spot due to the intense evaporation and ionization at that area [54, 56].

Even though HAVA is the cause for the anode material erosion phenomenon, but, the formation of HAVA is in fact influenced by the electrode geometry especially for the point-plane type geometry. Hence, when the electrode is a point-type geometry cathode, then the discharges are concentrated at the hot anode spot where the anode material erosion would take place [54, 56, 57, 95]. In this research, the electrode geometry used was in the form of cylinder-plane type, where the wire electrode was the cylinder-type electrode, while the workpiece was the plane-type electrode. Since the wire moves towards the workpiece using the *y*-axis, it is assumed that the concentration of the discharges at the hot anode spot is the same as the point-plane type geometry electrodes. Hence, when the wire electrode is cathode (negative polarity), then the discharges are concentrated at the hot anode spot which is dominated by the vacuum arcs that cause anode material removal [54, 56].

In contrast, based on Table 6 and Fig. 9, the unstable machining operation with high possibility of wire breakage happens when the workpiece polarity is negative with the lowest machining length of the microchannels (≤ 10 μm). The results are almost the same for both types of dielectric fluid: atmospheric air and compressed air. Since the polarity of the wire electrode is positive (anode), then it is expected that the

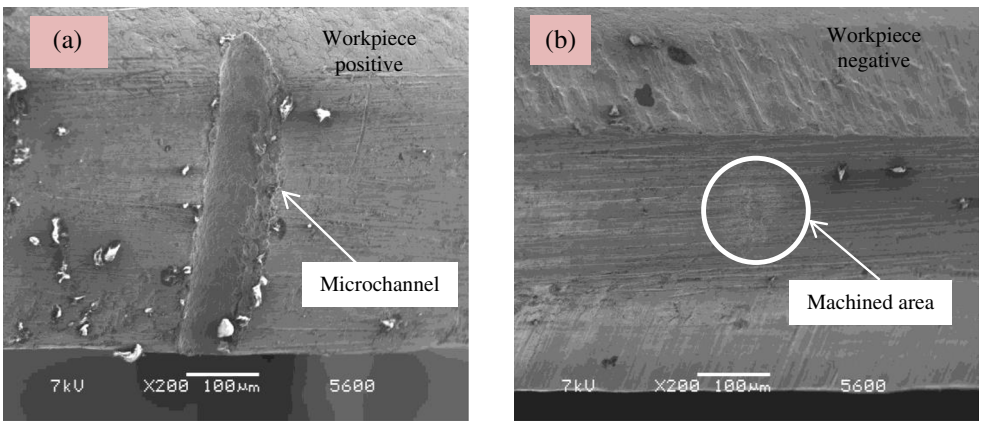

Fig. 8 SEM images for machined area of stainless steel machined with μDWEDM. Parameters: 90 V gap voltage, atmospheric air as dielectric fluid, 10 nF capacitance, 0.4 μm/s wire feed rate, 24% threshold, 0.0809 N wire tension, 0.5 rpm wire speed, and workpiece (**a**) positive and (**b**) negative polarity

Table 6 Experimental results for average machining length and standard deviation with different workpiece polarity

Workpiece polarity	Gap voltage (V)	Machining length (μm)			Average machining length (μm)	Standard deviation
		Trial 1	Trial 2	Trial 3		
Atmospheric air (0 MPa) (workpiece +ve)	80.00	64.80	35.30	40.00	46.70	15.85
	90.00	56.90	64.80	30.50	50.73	17.96
	100.00	51.50	41.80	15.70	36.33	18.52
	110.00	36.00	0.00	17.40	17.80	18.00
Atmospheric air (0 MPa) (workpiece −ve)	80.00	4.00	10.00	0.00	4.67	5.03
	90.00	0.00	6.00	0.00	2.00	3.46
	100.00	9.00	0.00	0.00	3.00	5.20
	110.00	10.00	5.00	0.00	5.00	5.00
Compressed air (0.0345 MPa) (workpiece +ve)	80.00	180.00	166.40	170.90	172.43	6.93
	90.00	300.00	286.40	295.60	294.00	6.94
	100.00	277.80	265.70	285.90	276.47	10.17
	110.00	181.60	197.80	205.70	195.03	12.29
Compressed air (0.0345 MPa) (workpiece −ve)	80.00	6.00	7.00	10.00	7.67	2.08
	90.00	0.00	10.00	0.00	3.33	5.77
	100.00	2.00	0.00	5.00	2.33	2.52
	110.00	4.00	0.00	0.00	1.33	2.31

possibility for the wire to break is high. It is because the wire wears increase since high material removal occurs when the electrode is anode (positive polarity). As a result, the material removed from the workpiece with negative polarity (cathode) is very low as shown in Fig. 8b. It can be concluded that the main cause for this condition to occur is due to the HAVA phenomenon as per discussed in the previous paragraph. Thus, based on the experimental results achieved, the best option to attain a stable and smooth machining operation for a cylinder-plane type geometry electrode is by using the workpiece as the positive polarity (anode), while the wire electrode was the negative polarity (cathode).

3.4 Threshold

Discharge between the two electrodes is generated when the electric strength reaches a certain breakdown threshold value that allows the dielectric fluid between the electrodes to act as an electrical conductor [11, 97, 104]. Figure 10 shows the SEM images with three different thresholds with constant parameters 90 V gap voltage, compressed air as dielectric fluid, workpiece positive polarity, 0.10 nF capacitance, 0.0345 MPa dielectric fluid pressure, 0.2 μm/s wire feed rate, 0.0809 N wire tension, and 0.6 rpm wire speed. Figure 10b, d, f shows the close-up SEM images at × 500 magnifications for Fig. 10a, c, e, respectively. From the figures, it shows that 24% threshold (Fig. 10c, d) gives the longest microchannel compared to the other two thresholds, 23% and 25%, since the material removal is the highest. Additionally, the similar outcome is also shown in Table 7 and Fig. 11 where 24% threshold is competent in producing longest microchannels, 285–300 μm, using μDWEDM. The experimental results for

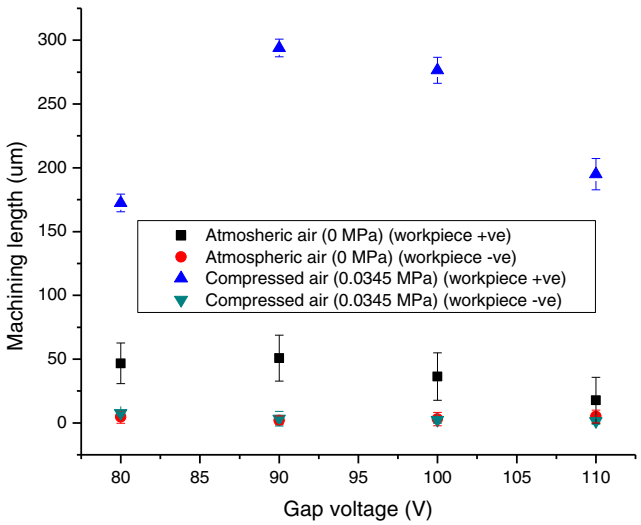

Fig. 9 Graph of machining length with respect to gap voltage for several combinations of dielectric fluid pressure and workpiece polarity as indicated by the legend. Atmospheric air (0 MPa) (workpiece +ve) gives higher machining length compared to atmospheric air (0 MPa) (workpiece −ve) with respect to gap voltage. Similar outcome is also shown when compressed air (0.0345 MPa) (workpiece +ve) is used compared to compressed air (0.0345 MPa) (workpiece −ve). Looking at these two combination, workpiece polarity has more significant role when the dielectric fluid pressure is higher. In the case of +ve polarity with high-pressure dielectric fluid, the machining is more sustainable. In the experimental results, the highest level of sustainability is found to be for 90–100 V gap voltage. Fixed parameters: 1 nF capacitance, 24% threshold, 0.2 μm/s wire feed rate, 0.0809 N wire tension, and 0.5 rpm wire speed

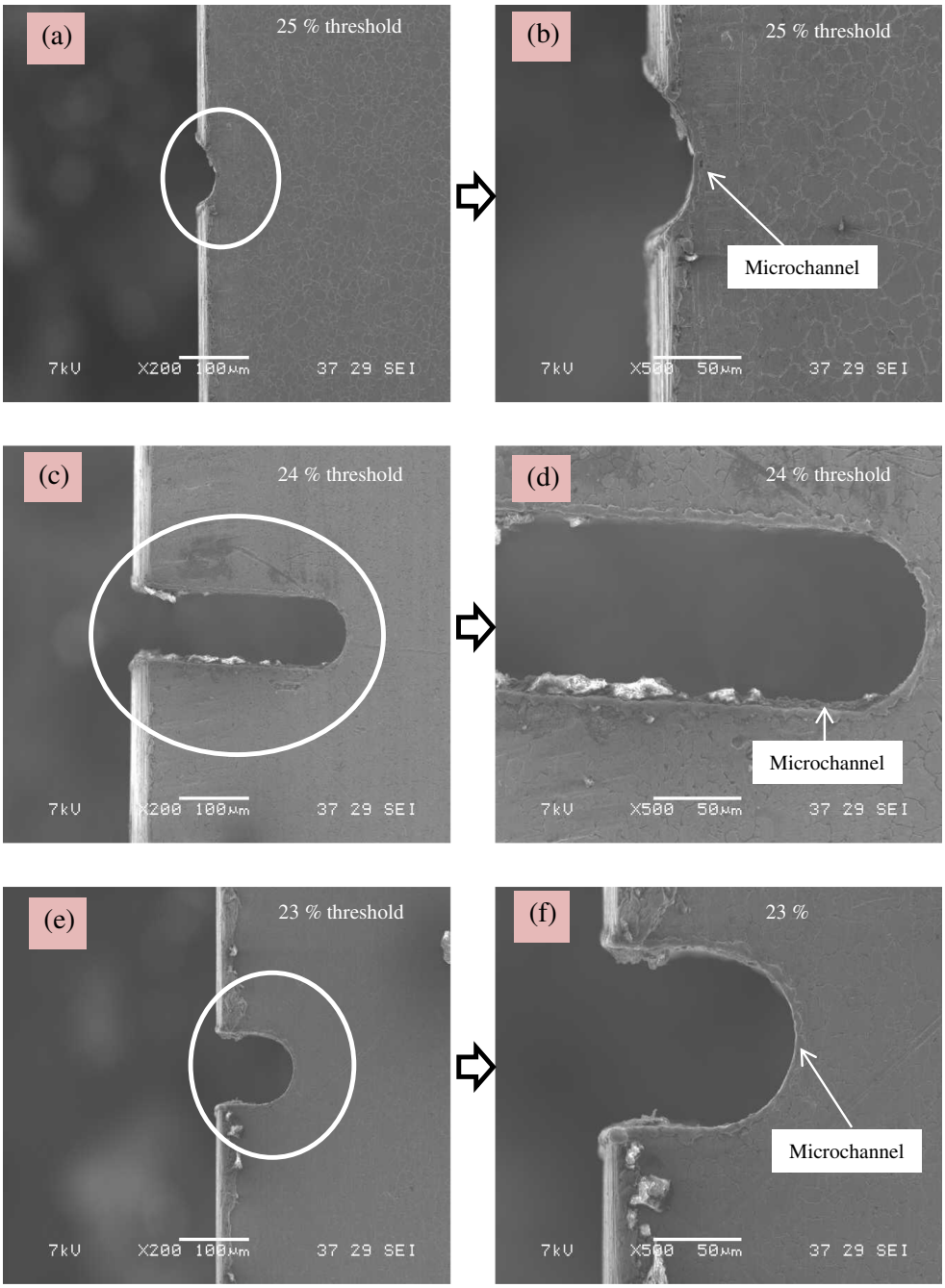

Fig. 10 SEM images for machined area of stainless steel machined with μDWEDM. Parameters: 90 V gap voltage, compressed air as dielectric fluid, workpiece positive polarity, 0.10 nF capacitance, 0.0345 MPa dielectric fluid pressure, 0.2 μm/s wire feed rate, 0.0809 N wire tension, 0.6 rpm wire speed, with (**a**), (**b**) 25%, (**c**), (**d**) 24%, (**e**), (**f**) 23% threshold; panels (**b**), (**d**), and (**f**) are the enlarged SEM images at × 500 magnification for panels (**a**), (**c**), and (**e**), respectively

the average machining length and standard deviation for different thresholds are tabulated in Table 7, while the scatter graph of the machining length with respect to gap voltage for threshold is shown in Fig. 11. The reason behind this incident is due to the gap distance between the electrodes, *d*, which is clarified by the modified Paschen's law.

According to the modified Paschen's law, the micro-breakdown voltage phenomenon for a particular gas composition is influenced by the gap distance between the electrodes, *d*, as discussed in the previous sections (Sects. 3.1 and 3.2). This is because when the gap distance of the electrodes is in microscale (< 10 μm in atmospheric air) and the breakdown voltage reaches minimum, then more energy is required to overcome the rapid loss of electrons in the microgap. As a result, the breakdown voltage will increase continuously [21, 29, 43, 46, 51, 54, 72, 85]. However, when the gap distance between the electrodes is less than 5 μm, microplasma production is possible if the voltage used is less than 300 V [82, 95] which is similar to this condition. In this occasion, it is assumed that the gap distance between the electrodes is less than 5 μm since the gap voltage used is less than 110 V. It is because the micro-breakdown mechanism is similar to the

Table 7 Experimental results for average machining length and standard deviation with three different thresholds

Threshold (%)	Gap voltage (V)	Machining length (μm)			Average machining length (μm)	Standard deviation
		Trial 1	Trial 2	Trial 3		
25	80.00	102.00	84.30	97.30	94.53	9.17
	90.00	90.50	96.80	104.00	97.10	6.75
	100.00	75.00	85.80	72.30	77.70	7.14
	110.00	66.30	73.00	63.70	67.67	4.80
24	80.00	285.30	300.00	300.00	295.10	8.49
	90.00	300.00	300.00	300.00	300.00	0.00
	100.00	300.00	295.60	300.00	298.53	2.54
	110.00	300.00	285.80	295.60	293.80	7.27
23	80.00	83.50	89.00	88.30	86.93	2.99
	90.00	94.50	92.30	84.80	90.53	5.09
	100.00	87.50	86.50	82.30	85.43	2.76
	110.00	63.30	56.30	67.00	62.20	5.43

vacuum breakdown since it consists of ion-enhanced field emission formation caused by the micro-protrusions on the cathode surface [54, 56, 77]. Moreover, ion-enhanced field emission in microgaps is initiated when there is a rapid fall of the breakdown voltage together with the decrement of the gap distance between the electrodes [78].

However, when the threshold is 25%, the machining length shown in Table 7 is between 63 and 104 μm. It indicates that the gap distance between the electrodes increases (it is assumed > 5 μm) which leads to the interruption of the micro-breakdown mechanism causing the machining operation to stop. Besides that, since the gap distance between the electrodes increases, higher voltage is required to generate the electric field threshold in order to create the micro-breakdown mechanism [63]. In contrast, when the threshold is 23%, the machining length shown in Table 7 is approximately 56 to 95 μm. It is caused by the poor flushing system where the generated debris is unable to leave the inter-electrode gap since the gap distance between the electrodes is too small. As a result, redundant sparks are produced since most of the generated spark energy is taken away by the debris causing the amount of the material removal to reduce [86]. As a conclusion, in order to produce microchannels with high amount of material removal, then the best option would be 24% threshold. However, it is needed to remember that the threshold value varies based on the type of gas used since the micro-breakdown mechanism differs based on different types of gas composition used.

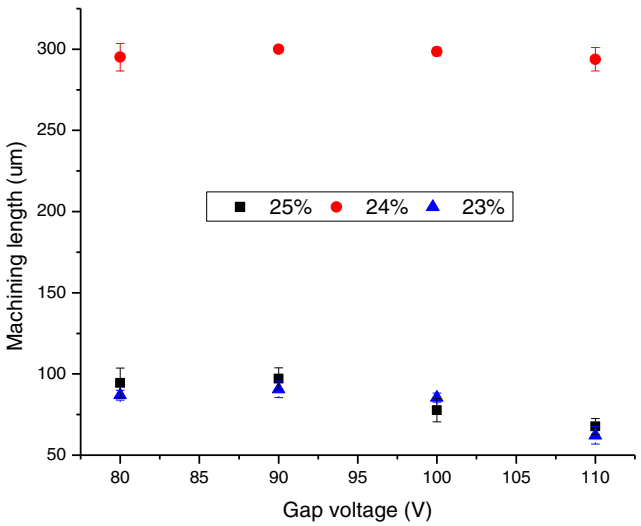

Fig. 11 Graph of machining length with respect to gap voltage for threshold as indicated by the legend. Threshold, 24%, gives the highest level of machining length compared to the other two thresholds, 23% and 25%, where the machining length is almost similar with respect to gap voltage. More sustainable machining is achievable when 24% threshold is used. Based on the experimental results, it shows that the highest level of sustainability is found to be for all of the values of the gap voltage. Fixed parameters: 1 nF capacitance, compressed air as dielectric fluid, 0.0345 MPa dielectric fluid pressure, workpiece positive polarity, 0.2 μm/s wire feed rate, 0.0809 N wire tension, and 0.6 rpm wire speed

3.5 Wire tension

Wire tension is a factor that controls the tension of the wire between the upper and lower wire guides where it has a significant effect on machining accuracy [8, 65, 70]. Normally, this parameter influences the wire vibration and wire lag during the machining operation [33, 34, 89] and sometimes can cause wire rupture if the applied tension is more than the wire tensile strength [69]. Figure 12 shows the SEM images of microchannels machined using μDWEDM for two different wire tension, 0.0809 N and 0.1214 N, with constant parameters 100 V gap voltage, compressed air as dielectric fluid, 1 nF capacitance, 0.0345 MPa dielectric fluid pressure, 0.2 μm/s wire feed rate, 24% threshold, workpiece positive polarity, and 0.6 rpm wire speed. Based on the SEM images, it shows that high amount of material is removed from the machined

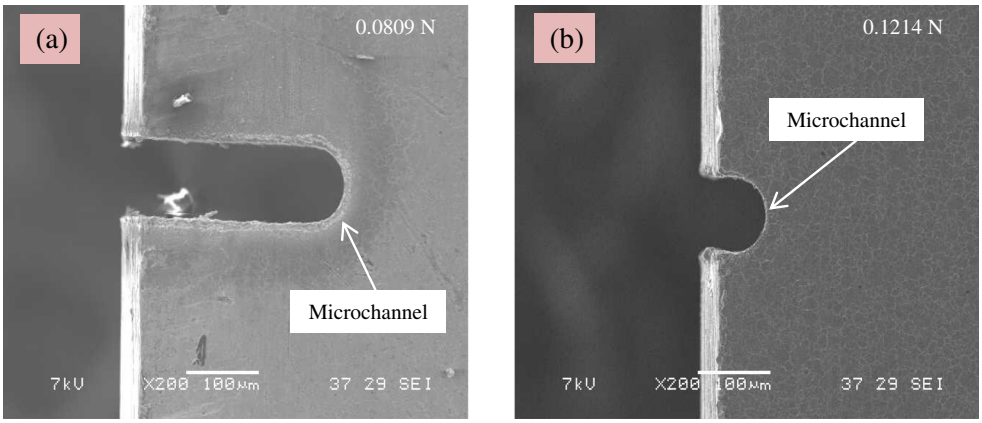

Fig. 12 SEM images for machined area of stainless steel machined with μDWEDM. Parameters: 100 V gap voltage, compressed air as dielectric fluid, 1 nF capacitance, 0.0345 MPa dielectric fluid pressure, 0.2 μm/s wire feed rate, 24% threshold, workpiece positive polarity, and 0.6 rpm wire speed, with wire tension of (**a**) 0.0809 N and (**b**) 0.1214 N

area in Fig. 12a when the wire tension is 0.0809 N compared to the Fig. 12b (0.1214 N wire tension). Similar outcome can be seen through Table 8 and Fig. 13 where Table 8 is the experimental results of the average machining length and standard deviation for two different wire tensions, while Fig. 13 is the scatter graph of the machining length with respect to gap voltage for wire tension. According to these figures and table, it is confirmed that stable and smooth machining operation with high amount of material removed is achievable when 0.0809 N wire tension is used. The average machining lengths for the microchannels were between 241 and 300 μm. However, wire breakage frequently occurred when the wire tension was 0.1214 N which is proven by the machining length of the microchannels, ≈41 to 111 μm, shown in Table 8 and Fig. 13. It is mainly caused by the wire vibration since wire tension and wire vibration are closely related to each other.

Apparently, when high wire tension is used, wire vibration will reduce [8, 96] since larger tension increases the wire's resistance to bend which brings the wire towards a balanced vibration pattern where the vibration amplitude is equal in both directions [96]. However, in this case, higher value of wire tension leads to wire breakage. It is due to the several forces acting on the wire during the machining operation: the reaction forces generated from the pressure of the gas bubbles during the erosion mechanism, hydrodynamic forces from the flushing system, the electrostatic forces that act on the wire, and the electromagnetic forces from the spark generation [17, 34, 59, 91]. But, for this investigation, the reaction force is negligible since no gas bubbles were generated during the erosion mechanism because the machining operation was done in dry condition [8, 27, 95]. Moreover, wire breakage also occurs due to high amount of stresses developed in wire caused by the wire properties and characteristics, cross-section reduction, and increment in wire temperature [69]. Therefore, for this investigation, it can be concluded that 0.0809 N wire

Table 8 Experimental results for average machining length and standard deviation with two different wire tensions

Wire tension (N)	Gap voltage (V)	Machining length (μm)			Average machining length (μm)	Standard deviation
		Trial 1	Trial 2	Trial 3		
0.0809	80.00	289.00	259.30	271.40	273.23	14.93
	90.00	300.00	300.00	295.30	298.43	2.71
	100.00	300.00	291.50	272.80	288.10	13.92
	110.00	250.70	241.70	262.60	251.67	10.48
0.1214	80.00	93.00	94.50	97.00	94.83	2.02
	90.00	95.00	84.50	108.00	95.83	11.77
	100.00	111.00	97.80	91.80	100.20	9.82
	110.00	60.00	41.80	47.50	49.77	9.31

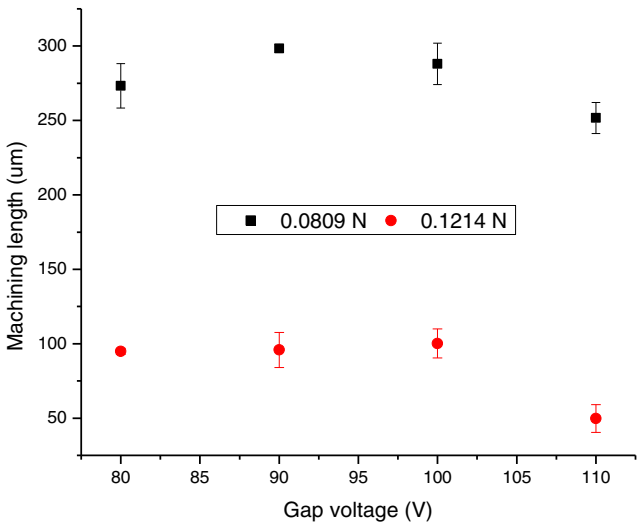

Fig. 13 Graph of machining length with respect to gap voltage for wire tension as indicated by the legend. Wire tension, 0.0809 N, gives highest machining length. The machining process is more sustainable with lower wire tension. The experimental results also showed that the machining has the highest level of sustainability when the 90–100 V gap voltage is used. Fixed parameters: 10 nF capacitance, compressed air as dielectric fluid, 0.0345 MPa dielectric fluid pressure, workpiece positive polarity, 24% threshold, 0.2 μm/s wire feed rate, and 0.6 rpm wire speed

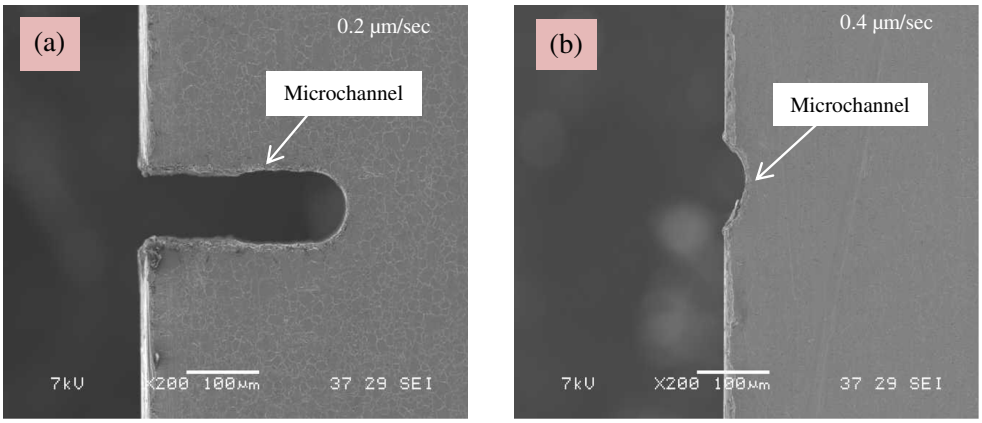

Fig. 14 SEM images for machined area of stainless steel machined with μDWEDM. Parameters: 90 V gap voltage, compressed air as dielectric fluid, 1 nF capacitance, 0.0345 MPa dielectric fluid pressure, 0.0809 N wire tension, 24% threshold, workpiece positive polarity, and 0.5 rpm wire speed, with (**a**) 0.2 μm/s and (**b**) 0.4 μm/s wire feed rate

tension is the best value to produce a smooth and stable machining operation with high amount of material removal.

3.6 Wire feed rate

Wire feed rate is a parameter where the wire electrode is fed continuously along the wire guide path towards the workpiece for continuous sparking [38, 69]. Figure 14 shows the SEM images for two different wire feed rate with fixed parameters 90 V gap voltage, compressed air as dielectric fluid, 1 nF capacitance, 0.0345 MPa dielectric fluid pressure, 0.0809 N wire tension, 24% threshold, workpiece positive polarity, and 0.5 rpm wire speed. Based on the figure, it shows that lower (0.2 μm/s) feed rate (Fig. 14a) gives better machining outcome compared to the 0.4 μm/s feed rate. The same results can also be seen through Table 9 and Fig. 15; Table 9 is the tabulated experimental results for average machining length and standard deviation for two different wire feed rate, while on the other hand, Fig. 15 is the scatter graph of machining length with respect to gap voltage for wire feed rate with fixed parameters 1 nF capacitance, 24% threshold, compressed air as dielectric fluid, 0.0345 MPa dielectric fluid pressure, workpiece positive polarity, 0.0809 N wire tension, and 0.5 rpm wire speed. Based on Table 9 and Fig. 15, it is verified that 0.2 μm/s wire feed rate gives the longest microchannels (≈ 207–300 μm) with high amount of material removal. In addition, the machining operation was smooth and stable with the wire electrode still in one piece when 0.2 μm/s wire feed rate was used.

However, when 0.4 μm/s wire feed rate was utilized during the machining operation, the results were totally opposite. On top of that, the wire electrode would easily break during the machining operation whenever the discharges are generated in the inter-electrode gap. In this situation, the wire breakage happens because the gap distance between the electrodes is gradually deteriorated [52]. As a result, it affects the micro-breakdown mechanism as per stated by the modified Paschen's law (Sects. 3.1 and 3.2). Even though the wire does not break instantaneously, but, the gap remains deteriorated until the wire breaks [52]. Besides that, chances for wire breakage are high when higher feed rate is used caused by the unwanted discharges that change the shape of the wire. The unwanted discharges are generated between the unflushed debris and the wire electrode [79]. Thus, 0.2 μm/s wire feed rate is recommended for this research for a smooth and stable machining operation.

Table 9 Experimental results for average machining length and standard deviation with two different wire feed rate

Wire feed rate (μm/s)	Gap voltage (V)	Machining length (μm)			Average machining length (μm)	Standard deviation
		Trial 1	Trial 2	Trial 3		
0.2	80.00	289.10	300.00	291.40	293.50	5.75
	90.00	300.00	296.70	300.00	298.90	1.91
	100.00	300.00	292.00	282.90	291.63	8.56
	110.00	214.00	226.70	207.50	216.07	9.77
0.4	80.00	116.00	127.00	123.00	122.00	5.57
	90.00	89.50	73.50	84.50	82.50	8.19
	100.00	97.80	82.30	79.80	86.63	9.75
	110.00	60.70	61.50	58.80	60.33	1.39

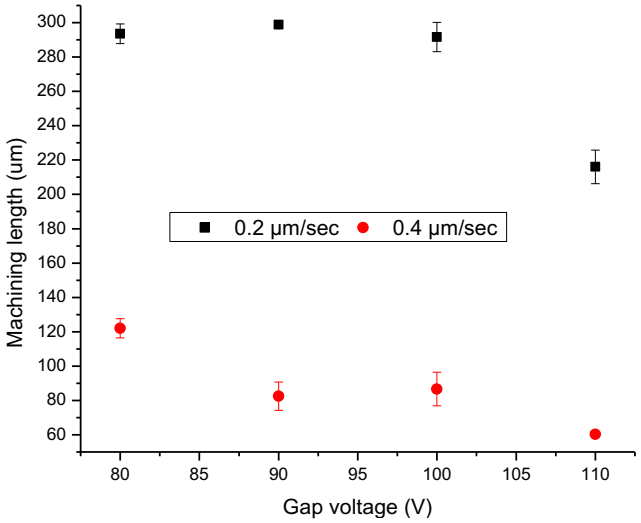

Fig. 15 Graph of machining length with respect to gap voltage for wire feed rate as indicated by the legend. Wire feed rate, 0.2 µm/s, gives higher machining length compared to the 0.4 µm/s with respect to gap voltage. The experimental results indicate that when wire feed rate is low, the machining process is more sustainable. The results also show that the highest level of sustainability is achievable when the gap voltage is between 80 and 100 V. Fixed parameters: 1 nF capacitance, 24% threshold, compressed air as dielectric fluid, 0.0345 MPa dielectric fluid pressure, workpiece positive polarity, 0.0809 N wire tension, and 0.5 rpm wire speed

3.7 Wire speed

Wire speed is a parameter that has impact on wire wear during the machining operation where it can lead to wire breakage [25, 28]. Figure 16 shows the SEM images of microchannels for different wire speed, 0.5 rpm and 0.6 rpm, with constant parameters 90 V gap voltage, compressed air as dielectric fluid, 0.10 nF capacitance, 0.0345 MPa dielectric fluid pressure, 0.0809 N wire tension, 24% threshold, workpiece positive polarity, and 0.2 µm/ s feed rate. Moreover, the experimental results for average machining length and standard deviation for different wire speed are tabulated in Table 10, while the scatter graph of machining length with respect to gap voltage for wire speed is shown in Fig. 17. Based on Fig. 16, high amount of material is removed when 0.6 rpm wire speed is used during the machining operation (Fig. 16b) compared to 0.5 rpm wire speed (Fig. 16a). The same outcome is shown in Table 10 and Fig. 17 where the machining lengths of the microchannels were approximately 228 to 280 µm when 0.6 rpm wire speed was used. However, when 0.5 rpm wire speed was utilized, the machining lengths for the microchannels were around 74 to 106 µm. In addition, whenever 0.5 rpm wire speed was used, the wire would easily break off after a few discharges occurred between the wire and the workpiece at the inter-electrode gap.

It is known that µWEDM is a machining operation that removes the material by thermal energy created by the electrical discharges [36, 73, 74]. However, the material removal mechanism in this type of machining operation happens in both of the electrodes: wire electrode and workpiece [58]. The small amount of materials removed from the wire is the cause for the wire to wear resulting in wire breakage since the stresses developed in the wire are more than the wire strength [69]. In addition, wire speed is also interrelated with wire vibration during the machining operation. However, wire speed affects the frequency of the wire vibration not the maximum amplitude [101]. Therefore, as a solution, high wire speed (0.6 rpm wire speed) is suggested to be used during the machining operation since fresh wire is continuously supplied in order to avoid high amount of stresses developed at one point.

3.8 Capacitance

Capacitance is a capability of storing the electrical charge in its electric field. It is actually a ratio of the charge on one plate of a capacitor to voltage difference between two plates [4]. In this section, the experimental results for the average machining length and standard deviation using different capacitance are tabulated in Table 11. Meanwhile, Fig. 18 is the scatter

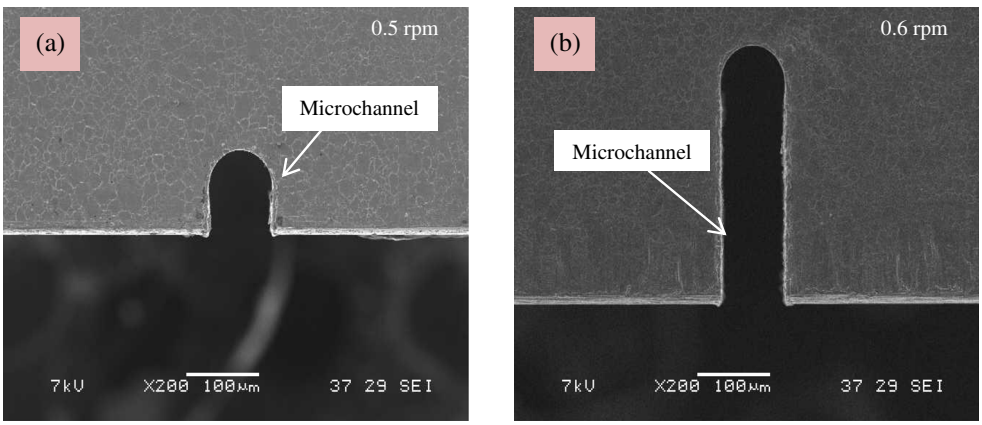

Fig. 16 SEM images for machined area of stainless steel machined with µDWEDM. Parameters: 90 V gap voltage, compressed air as dielectric fluid, 0.10 nF capacitance, 0.0345 MPa dielectric fluid pressure, 0.0809 N wire tension, 24% threshold, workpiece positive polarity, and 0.2 µm/s wire feed rate, with (**a**) 0.5 rpm and (**b**) 0.6 rpm wire speed

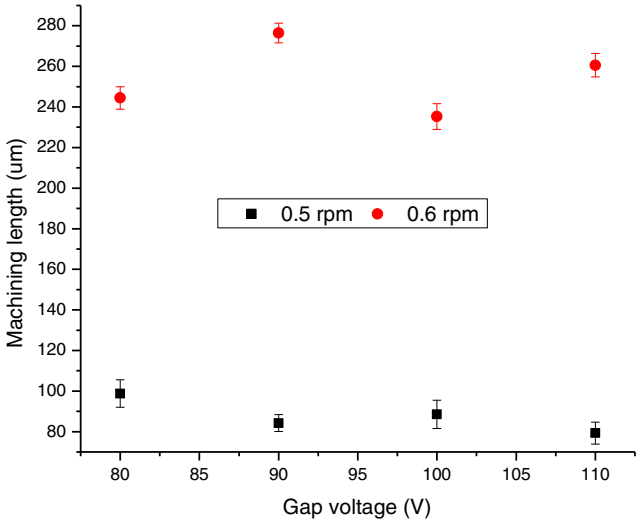

Fig. 17 Graph of machining length with respect to gap voltage for wire speed as indicated by the legend. Wire speed, 0.6 rpm, gives higher machining length compared to 0.5 rpm with respect to gap voltage. In the experimental results, machining process is more sustainable when high wire speed is used. It was also found that the highest sustainability is achievable at 90 V gap voltage. Fixed parameters: 0.10 nF capacitance, 24% threshold, compressed air as dielectric fluid, 0.0345 MPa dielectric fluid pressure, workpiece positive polarity, 0.0809 N wire tension, and 0.2 μm/s wire feed rate

graph of the machining length with respect to gap voltage for capacitance. Based on the table and the figure, it shows that when 100 nF and 0.01 nF are used, the material removed during the machining operation are small since the machining length for the microchannels is less than 143 μm. Furthermore, when 100 nF capacitance is utilized, the wire would easily break during the machining operation. This is because when high amount of capacitance is used, high discharge energy is produced where stronger sparks are generated to erode more material. However, due to the material erosion, there is unflushed debris trapped at the inter-electrode gap which can lead to the unwanted sparks between the tool and the debris. As a result, low amount of material is removed

Table 10 Experimental results for average machining length and standard deviation with two different wire speed

Wire speed (rpm)	Gap voltage (V)	Machining length (μm)			Average machining length (μm)	Standard deviation
		Trial 1	Trial 2	Trial 3		
0.5	80.00	106.00	92.50	97.80	98.77	6.80
	90.00	79.90	88.30	84.50	84.23	4.21
	100.00	82.30	87.20	96.00	88.50	6.94
	110.00	84.70	79.10	74.00	79.27	5.35
0.6	80.00	239.80	250.60	242.90	244.43	5.56
	90.00	280.00	278.30	270.90	276.40	4.84
	100.00	228.40	236.70	240.80	235.30	6.32
	110.00	255.90	267.00	258.80	260.57	5.76

Table 11 Experimental results for average machining length and standard deviation with different capacitance

Capacitance (nF)	Gap voltage (V)	Machining length (μm)			Average machining length (μm)	Standard deviation
		Trial 1	Trial 2	Trial 3		
100	80.00	100.00	113.00	109.80	107.60	6.77
	90.00	118.80	128.70	131.00	126.17	6.48
	100.00	138.00	143.80	125.80	135.87	9.19
	110.00	94.50	103.80	105.70	101.33	5.99
10	80.00	256.00	264.80	255.00	258.60	5.39
	90.00	286.80	295.00	300.00	293.93	6.66
	100.00	300.00	293.90	300.00	297.97	3.52
	110.00	290.00	291.90	300.00	293.97	5.31
1.00	80.00	300.00	294.00	289.60	294.53	5.22
	90.00	295.00	300.00	300.00	298.33	2.89
	100.00	300.00	287.90	296.20	294.70	6.19
	110.00	278.90	291.90	281.00	283.93	6.98
0.10	80.00	290.00	287.30	279.80	285.70	5.28
	90.00	294.30	290.40	300.00	294.90	4.83
	100.00	300.00	300.00	289.00	296.33	6.35
	110.00	297.00	288.70	289.80	291.83	4.51
0.01	80.00	96.80	98.60	86.70	94.03	6.41
	90.00	86.00	83.80	76.90	82.23	4.75
	100.00	71.00	80.90	76.90	76.27	4.98
	110.00	73.90	79.70	80.90	78.17	3.74

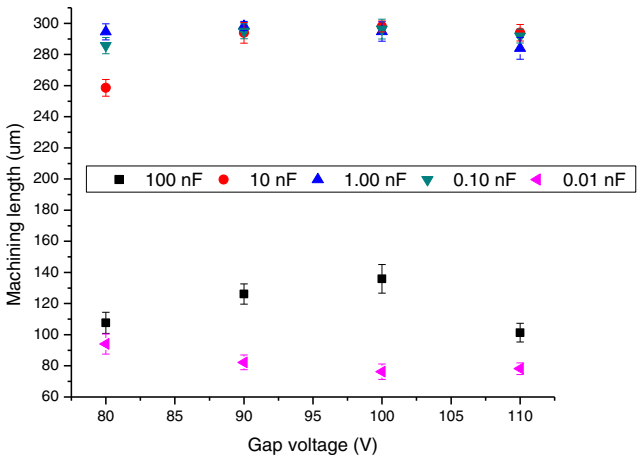

Fig. 18 Graph of machining length with respect to gap voltage for capacitance as indicated by the legend. Highest level machining length is achievable when 10 nF, 1.00 nF, and 0.10 nF capacitance is used with respect to the gap voltage. On the other hand, the machining length is at the lowest when 0.01 nF capacitance is used. As for the 100 nF capacitance, the machining length is slightly above from the results of 0.01 nF capacitance. Looking at the results, it shows that the value of the capacitance has significant impact on the sustainability of the machining process. The machining process is sustainable for all of the values of the gap voltage. Fixed parameters: 24% threshold, compressed air as dielectric fluid, 0.0345 MPa dielectric fluid pressure, workpiece positive polarity, 0.0809 N wire tension, 0.2 μm/s wire feed rate, and 0.6 rpm wire speed

Table 12 Experimental results for average machining length and standard deviation for different gap voltage

Gap voltage (V)	Machining length (μm)			Average machining length (μm)	Standard deviation
	Trial 1	Trial 2	Trial 3		
80.00	300.00	295.60	289.80	295.13	5.12
90.00	300.00	294.90	300.00	298.30	2.94
100.00	297.80	289.70	300.00	295.83	5.42
110.00	286.40	287.60	294.70	289.57	4.49

from the workpiece [79]. Moreover, wire vibration increases when the discharge energy is high which may cause wire breakage [8]. Conversely, when too small capacitance (0.01 nF) is used, the discharge energy produce is not enough to generate the micro-breakdown voltage mechanism. Thus, for a smooth and stable machining, it is recommended to use capacitance of 10 nF, 1.00 nF, and 0.10 nF.

3.9 Gap voltage

As for the gap voltage, smooth and stable machining operation with wire still in one piece is possible for all the varied values which are shown in Table 12 and Fig. 19. Table 12 shows the experimental results for average machining length and standard deviation for different gap voltage, while Fig. 19 shows the scatter graph of the machining length with respect to gap voltage. The average machining length for these gap voltages was within 286 to 300 μm. This situation is due to the generation of microplasma which involves the micro-breakdown phenomenon as per discussed in the previous sections (Sects. 3.2, 3.3, and 3.4). The phenomenon is developed once there is a sufficiently high electric field to accelerate the electrons [50, 77, 85, 90]. Normally, gap voltage influences the formation of the electric field [9, 22, 23, 47]. Therefore, all the values—80 V, 90 V, 100 V, and 110 V—of the gap voltage are capable in providing a smooth and stable machining operation.

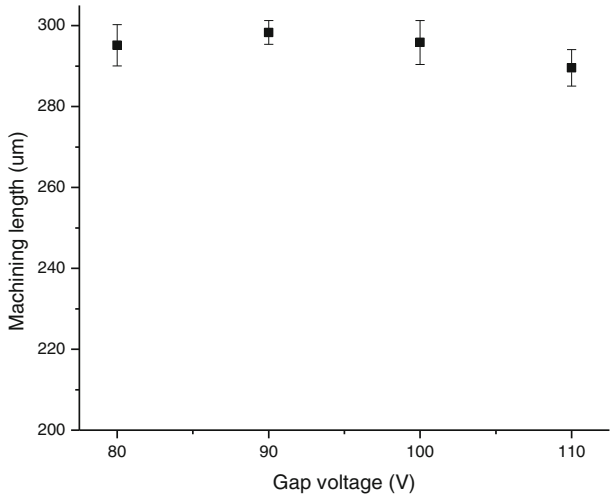

Fig. 19 Graph of machining length with respect to gap voltage. All of the values of the gap voltage gives more than 280 μm machining length. The machining process is sustainable for 80–110 V gap voltage. Fixed parameters: 1 nF capacitance, 24% threshold, compressed air as dielectric fluid, 0.0345 MPa dielectric fluid pressure, workpiece positive polarity, 0.0809 N wire tension, 0.2 μm/s wire feed rate, and 0.5 rpm wire speed

4 Conclusions

In this research, μDWEDM was introduced as a potential fabrication technique in order to produce features with high accuracy and precision. The parameters such as types of dielectric fluid, dielectric fluid pressure, workpiece polarity, threshold, wire tension, wire feed rate, wire speed, gap voltage, and capacitance were carefully identified to achieve a stable machining operation. During this phase, the experimentation method used was a conventional experimental method which was OFAT. The results were based on the SEM images and the scatter graphs of the microchannels machined by μDWEDM. This research showed the following:

1. Process parameters such as types of dielectric fluid, dielectric fluid pressure, workpiece polarity, threshold, wire tension, wire feed rate, wire speed, gap voltage, and capacitance for uninterrupted, stable, and smooth μDWEDM process have been identified. Previously, these parameters and their level of influences were unknown, and smooth and stable μDWEDM process was not possible which eventually hinders the industrial applications. This investigation opens the door for μDWEDM for industrial application.
2. Stable and smooth machining operation is attainable when compressed air was used as the dielectric fluid, 0.0345 MPa dielectric fluid pressure, workpiece positive polarity, 24% threshold, 0.0809 N wire tension, 0.2 μm/s wire feed rate, and 0.6 rpm wire speed. It was proposed that capacitance (10 nF, 1.00 nF, and 0.10 nF) and gap voltage (80 to 110 V) should be used for further investigation.
3. The fundamental reason for a stable and smooth μDWEDM process is explainable by the formation of the micro-breakdown phenomenon as mentioned by the modified Paschen's law.
4. μDWEDM is a new research area in the field of micromachining; as such, there is no extensive research results that have been reported. As such, a comprehensive benchmarking is not possible. The findings are benchmarked with Hoang and Yang [36], Macedo et al. [54], and Macedo et al. [57], as described below.

(a) Dielectric fluid pressure is found to have impact on the gap distance between the electrodes which is similar with [37].
(b) Workpiece positive polarity is found to have impact on the material removal as mentioned by the previous study on DEDM [56].
(c) EDM usually used workpiece positive and tool negative polarity although opposite polarity is not uncommon for specific cases. Our study on the regular polarity (workpiece positive and tool negative) is found to be effective. Macedo et al. [57] also found that regular polarity is more effective for DEDM.

5. It is recommended that different types of gases should be used for detailed investigation related to the accuracy of the μDWEDM. This is because micro-breakdown mechanism differs based on different types of gas composition used.

Acknowledgements The authors are thankful to faculty and staff at Micromanufacturing Laboratory and Metallographic Laboratory at IIUM for their support.

Funding information This research was funded by MOSTI, under Research Grant SF15-016-0066.

References

1. Abbas MN, Solomon DG, Fuad Bahari M (2007) A review on current research trends in electrical discharge machining (EDM). Int J Mach Tools Manuf 47(7):1214–1228
2. Ahmad M (2007) An experimental investigation of single and multi-tool micro-EDM (master's thesis). National University of Singapore, Singapore
3. Akkurt A (2009) Surface properties of the cut face obtained by different cutting methods from AISI 304 stainless steel materials. Indian J Eng Mater Sci 16:373–384
4. Alexander CK, Sadiku MNO (2007) Fundamentals of electric circuits. New York, US: McGraw-Hill Higher Education
5. Ali MY, Hung WNP (2017) Micromachining. In: Hashmi MSJ (ed) Comprehensive materials finishing, vol 1. Elsevier, Oxford, pp 322–323
6. Ali MY, Mohammad AS (2008) Experimental study of conventional wire electrical discharge machining for microfabrication. Mater Manuf Process 23:641–645
7. Ali MY, Karim ANM, Adesta EYT, Ismail AF, Abdullah AA, Idris MN (2010) Comparative study of conventional and micro WEDM based on machining of meso/micro sized spur gear. Int J Precis Eng Manuf 11(5):779–784
8. Ali MY, Banu A, Salehan M, Adesta EYT, Hazza M, Shaffiq M (2018) Dimensional accuracy in dry micro wire electrical discharge machining. J Mech Eng Sci 12(1):3321–3329
9. Alias A, Abdullah B, Abbas NM (2012) Influence of machine feed rate in WEDM of titanium Ti-6Al-4V with constant current (6A) using brass wire. Procedia Eng 41:1806–1811
10. Azhiri RB, Teimouri R, Baboly MG, Laseman Z (2014) Application of Taguchi, ANFIS and grey relational analysis for studying, modelling and optimization of wire EDM process while using gaseous media. Int J Adv Manuf Technol 71(1):279–295
11. Bada J (2011) Spark discharge. In: Gargaud M, Amils R, Cleaves HJ (eds) Encyclopedia of astrobiology, vol 1. Springer, Berlin
12. Bahru Stainless (2017) Inspection certificate 3.1. Retrieved from Bahru Stainless
13. Banu A, Ali MY (2016) Electrical discharge machining (EDM): a review. Int J Eng Mater Manuf 1(1):3–10
14. Besliu I, Coteata M (2009) Characteristics of the dry electrical discharge machining. Nonconv Technol Rev 2:5–8
15. Chen YF, Lin YC, Chen SL, Hsu LR (2009) Optimization of electrodischarge machining parameters on ZrO_2 ceramic using the Taguchi method. J Eng Manuf 224:195–205
16. Chow HM, Yang LD, Lin CT, Chen YF (2008) The use of SiC powder in water as dielectric for micro-slit EDM machining. J Mater Process Technol 195(1–3):160–170
17. Conde A, Arriandiaga A, Sanchez JA, Portillo E, Plaza S, Canabes I (2018) High-accuracy wire electrical discharge machining using artificial networks and optimization techniques. Robot Comput Integr Manuf 49:24–38
18. Davim JP (2017) Microfabrication and precision engineering: research and development. Elsevier, Woodhead Publishing
19. Descoeudres A (2006) Characterization of electrical discharge machining plasmas (doctor of philosophy's dissertation). Ecole Polytechnique Federale De Lausanne, Lausanne
20. Dhakar K, Dvivedi A (2016) Parametric evaluation on near-dry electric discharge machining. Mater Manuf Process 31:413–421
21. Dhariwal RS, Torres JM, Desmulliez MPY (2000) Electric field breakdown at micrometer separations in air and nitrogen at atmospheric pressure. IEE Proc Sci Meas Technol 147(5):261–265
22. Faircloth DC (2014) Technological aspects: high voltage. Retrieved from http://arxiv.org/ftp/arxiv/papers/1404/1404.0952.pdf (2018, April 9)
23. Florkowska B, Florkowski M, Roehrich J, Zydron P (2010) Partial discharge mechanism in a non-uniform electric field at higher pressure. IET Sci Meas Technol 5(2):59–66
24. Frohn-Villeneuve L, Curodeau A (2013) Dry die-sinking EDM with mouldable graphite-polymer electrode investigation of process parameters and pulse identification methods. Int J Adv Manuf Technol 65(5–8):1125–1139
25. Garg RK, Singh KK, Sachdeva A, Sharma VS, Ojha K, Singh S (2010) Review of research work in sinking EDM and WEDM on metal matrix composite materials. Int J Adv Manuf Technol 50(5–8):611–624
26. Garson GD (2012) Testing statistical assumptions. Statistical Associates Publishing, Asheboro
27. Ghodsiyeh D, Moradi M (2015) Wire electrical discharge machining. In: Jahan MP (ed) Electrical discharge machining (EDM) types, technologies and applications. Nova Science Publishers, Inc., New York, pp 33–65
28. Ghodsiyeh D, Golshan A, Shirvanehdeh JA (2013) Review on current research trends in wire electrical discharge machining (WEDM). Indian J Sci Technol 6(2):4128–4140
29. Go DB, Pohlman DA (2010) A mathematical model of the modified Paschen's curve for breakdown in microscale gaps. J Appl Phys 107(10):103303
30. Goodarzia G, Dehghani S, Akbarzadeh A, Date A (2017) Energy saving opportunities in air drying process in high-pressure compressors. Energy Procedia 110:428–433
31. Goodhew PJ, Humphreys J, Beanland R (2000) Electron microscopy and analysis. New York, US: CRC Press
32. Govindan P, Gupta A, Joshi SS, Malshe A, Rajurkar KP (2013) Single-spark analysis of removal phenomenon in magnetic field assisted dry EDM. J Mater Process Technol 213(7):1048–1058
33. Habib S, Okada A (2016) Experimental investigation on wire vibration during fine wire electrical discharge machining process. Int J Adv Manuf Technol 84(9–12):2265–2276

34. Ho KH, Newman ST, Rahimifard S, Allen RD (2004) State of the art in wire electrical discharge machining (WEDM). Int J Mach Tools Manuf 44:1247–1259
35. Hoang KT, Yang SH (2013) A study on the effect of different vibration-assisted methods in micro-WEDM. J Mater Process Technol 213:1616–1622
36. Hoang KT, Yang SH (2015a) A new approach for micro-WEDM control based on real-time estimation of material removal rate. Int J Precis Eng Manuf 16(2):241–246
37. Hoang KT, Yang SH (2015b) Kerf analysis and control in dry micro-wire electrical discharge machining. Int J Adv Manuf Technol 78:1803–1812
38. John D (2011) Multi response optimization of wire electric discharge machining with analytic hierarchy process (master's thesis). Thapar University, Patiala, Punjab
39. Kapoor J, Singh S, Khamba JS (2012) High-performance wire electrodes for wire electrical-discharge machining—a review. Proc Inst Mech Eng B J Eng Manuf 226(11):1757–1773
40. Kawata A, Okada A, Okamoto Y, Kurihara H (2017) Influence of nozzle jet flushing on wire breakage in 1st-cut wire EDM from start hole. Key Eng Mater 749:130–135
41. Khan DA, Hameedullah M (2011) Effect of tool polarity on the machining characteristics in electrical discharge machining of silver steel and statistical modelling of the process. Int J Eng Sci Technol 3(6):5001–5010
42. Khatri BC, Rathod PP (2017) Investigations on the performance of concentric flow dry wire electric discharge machining (WEDM) for thin sheets of titanium alloy. Int J Adv Manuf Technol 92(5–8): 1945–1954
43. Klas M, Matejcik S, Radjenovic B, Radmilovic-Radjenovic M (2011a) Experimental and theoretical studies of the breakdown voltage characteristics at micrometer separations in air. EPL (Europhys Lett) 95(3):35002
44. Klas M, Matejcik S, Radjenovic B, Radmilovic-Radjenovic M (2011b) Experimental and theoretical studies of direct-current breakdown voltage in argon at micrometer separations. Phys Scr 83(4):045503
45. Klas M, Matejcik S, Moravsky L, Radjenovic B, Radmilovic-Radjenovic M (2017a) Field-emission enhanced breakdown in oxygen microdischarges from direct-current to radio-frequencies. EPL (Europhys Lett) 120(2):25002
46. Klas M, Moravsky L, Matejcik S, Zahoran M, Martisovits V, Radjenovic B, Radmilovic-Radjenovic M (2017b) The breakdown voltage characteristics of compressed ambient air microdischarges ffrom direct current to 10.2 MHz. Plasma Sources Sci Technol 26(5):055023
47. Kuffel E, Zaengl WS, Kuffel J (2000) High voltage engineering fundamentals, 2nd edn. Butterworth-Heinemann, Great Britain
48. Kunieda M, Furudate C (2001) High precision finish cutting by dry WEDM. CIRP Ann Manuf Technol 50(1):121–124
49. Kunieda M, Lauwers B, Rajurkar KP, Schumacher BM (2005) Advancing EDM through fundamental insight into the process. CIRP Ann Manuf Technol 54(2):64–87
50. Li Y (2014) Analysis of ion-enhanced field emission and field emission-driven microdischarges (doctor of philosophy's dissertation). Notre Dame University, Notre Dame, Indiana
51. Li Y, Tirumala R, Rumbach P, Go DB (2013) The coupling of ion-enhanced field emission and the discharge during microscale breakdown at moderately high pressures. IEEE Trans Plasma Sci 41(1):24–35
52. Liao YS, Chu YY, Yan MT (1997) Study of wire breaking process and monitoring of WEDM. Int J Mach Tools Manuf 37(4):555–567
53. Liqing L, Yingjie S (2013) Study of dry EDM with oxygen-mixed and cryogenic cooling approaches. Procedia CIRP 6:344–350
54. Macedo FTB, Wiessner M, Hollenstein C, Esteves PMB, Wegener K (2016) Fundamental investigation of dry electrical discharge machining (DEDM) by optical emission spectroscopy and its numerical interpretation. Int J Adv Manuf Technol 90(9-12):3697–3709
55. Macedo FTB, Wiessner M, Hollenstein C, Kuster F, Wegener K (2016a) Dependence of crater formation in dry EDM on electrical breakdown mechanism. Procedia CIRP 42:161–166
56. Macedo FTB, Wiessner M, Hollenstein C, Kuster F, Wegener K (2016b) Investigation of the fundamentals of tool electrode wear in dry EDM. Procedia CIRP 46:55–58
57. Macedo FTB, Wiessner M, Bernardelli GC, Kuster F, Wegener K (2018) Fundamental investigation of EDM plasmas, part II: parametric analysis of electric discharges in gaseous dielectric medium. Procedia CIRP 68:336–341
58. Maher I, Sarhan AAD, Hamdi M (2015) Review of improvements in wire electrode properties for longer working time and utilization in wire EDM machining. Int J Adv Manuf Technol 76:329–351
59. Maradia U, Wegener K (2015) EDM modelling and simulation. In: Jahan MP (ed) Electrical discharge machining (EDM) types, technologies and applications. Nova Science Publishers, Inc., New York, pp 67–121
60. Micheli L, Reddy KS, Mallick TK (2015) Plate micro-fins in natural convection: an opportunity for passive concentrating photovoltaic cooling. Energy Procedia 82:301–308
61. Miller HC (1997) Anode modes in vacuum arcs. IEEE Trans Dielectr Electr Insul 4(4):382–388
62. Montgomery DC (2012) Design and analysis of experiments, 8th edn. Wiley, New York
63. Mujumdar SS, Curreli D, Kapoor SG (2016) Effect of dielectric electrical conductivity on the characteristics of micro electro-discharge machining plasma and material removal. J Micro Nano-Manuf 4(2):021006
64. Munz M, Risto M, Haas R (2016) The phenomenon of polarity in EDM drilling process using water based dielectrics. Procedia CIRP 42:532–536
65. Nayak BB (2015) Parametric optimization of taper cutting process using wire electrical discharge machining (WEDM) (doctoral's thesis). National Institute of Technology, Rourkela
66. Pal VK, Choudhury SK (2014) Fabrication and analysis of micro-pillars by abrasive water jet machining. Procedia Mater Sci 6:61–71
67. Pandey AB, Brahmankar PK (2016) A method to predict possibility of arcing in EDM of TiB_2p reinforced ferrous matrix composite. Int J Adv Manuf Technol 86(9–12):2837–2849
68. Pandey A, Singh S (2010) Current research trends in variants of electrical discharge machining: a review. Int J Eng Sci Technol 2(6):2172–2191
69. Patel VD, Patel DM, Patel UJ, Patel B, Butani N (2014) Review of wire-cut EDM process on titanium alloy. Int J Eng Res Appl 4(12):112–121
70. Patil PA, Waghmare CA (2014) A review on advances in wire electrical discharge machining. In: Proceedings of the International Conference on Research and Innovation in Mechanical Engineering. Springer, India, pp 179–189
71. Paul G, Roy S, Sarkar S, Hanumaiah N, Mitra S (2013) Investigations on influence of process variables on crater dimensions in micro-EDM of titanium aluminide alloy in dry and oil dielectric media. Int J Adv Manuf Technol 65:1009–1017
72. Peschot A, Bonifaci N, Lesaint O, Valadares C, Poulain C (2014) Deviations from the Paschen's law at short gap distances from 100 nm to 10 μm in air and nitrogen. Appl Phys Lett 105(12): 123109
73. Pour GT, Pour YT, Ghoreishi M (2014a) Thermal model of the electro-spark nanomachining process. Int J Mater Mech Manuf 2(1):56–59

74. Pour GT, Pour YT, Ghoreishi M (2014b) Electro-spark nanomachining process simulation. Int J Mater Mech Manuf 2(1):56–59
75. Pradeep GM, Dani MSH (2015) A review on the use of pollution free dielectric fluids in wire electrical discharge machining process. J Chem Pharm Sci 7:312–315
76. Puri AB (2017) Advancements in micro wire-cut electrical discharge machining. In: Non-traditional micromachining processes. Cham, Switzerland: Springer International Publishing, pp 145–178
77. Radmilovic-Radjenovic M, Radjenovic B (2017) The effect of the field emission on the breakdown voltage characteristics of nitrogen microdischarges. Int J Eng Innov Res 6(6):280–283
78. Radmilovic-Radjenovic M, Radjenovic B, Klas M, Bojarov A, Matejcik S (2013) The breakdown mechanisms in electrical discharges: the role of the field emission effect in direct current discharges in microgaps. Acta Phys Slovaca 63(3):105–205
79. Reyad M, Ali MY (2009) Investigation of machining parameters for multiple-response optimization of micro electrodischarge milling. Int J Adv Manuf Technol 43(3–4):264–275
80. Reza MS, Azmir MA, Tomadi SH, Hassan MA, Daud R (2010) Effects of polarity parameter on machining of tool steel workpiece using electrical discharge machining. In: Proceedings of the National Conference in Mechanical Engineering Research and Postgraduate Students, Kuantan, Pahang, Malaysia, pp 26–27
81. Richert MW, Boczkal G, Hotlos A, Palka P, Karpinski M (2017) Tribological wear behavior of electrical contacts made from AgNi10 composite. Arch Metall Mater 62(4):2007–2013
82. Roth R, Balzer H, Kuster F, Wegener K (2012) Influence of the anode material on the breakdown behavior in dry electrical discharge machining. Procedia CIRP 1:639–644
83. Rumbach P, Go DB (2012) Fundamental properties of field emission-driven direct current microdischarges. J Appl Phys 112(10):103302
84. Rumbachk P, Li Y, Martinez S, Twahirwa TJ, Go DB (2014) Experimental study of electron impact ionization in field emission-driven microdischarges. Plasma Sources Sci Technol 23(6):065026
85. Sawyer J, Abboud J, Zhang Z, Adams SF (2015) Reduction of breakdown threshold by metal nanoparticle seeding in a DC microdischarge. Nanoscale Res Lett 10(1):15
86. Saxena KK, Srivastava AS, Agarwal S (2016) Experimental investigation into the micro EDM characteristics of conductive SiC. Ceram Int 42(1):1597–1610
87. Schulze HP (2017) Importance of polarity change in the electrical discharge machining. In: AIP Conference Proceedings 1896(1): 050001
88. Singh P, Chaudhary AK, Singh T, Rana AK (2015) Comparison of outputs for dry EDM and EDM with oil: a review. Int J Res Emerg Sci Technol 2(6):45–49
89. Singu SMR, Reddy KH, Venkatarao K, Rao CVSP (2017) Experimental investigations on wire vibration, spark gap, MRR and surface roughness in WEDM for HC-HCR steel. Int J Mech Eng Technol 8(8):127–139
90. Tan X, Go DB (2018) Understanding the scaling of electron kinetics in the transition from collisional to collisionless conditions in microscale gas discharges. J Appl Phys 123(6):063303
91. Tomura S, Kunieda M (2009) Analysis of electromagnetic force in wire-EDM. Precis Eng 33:255–262
92. Vernon-Parry KD (2000) Scanning electron microscopy: an introduction. III-Vs Rev 13(4):40–44
93. Wang T, Kunieda M (2004) Dry WEDM for finish cut. Key Eng Mater 259-260:562–566
94. Wang T, Xie SQ, Xu XC, Chen Q, Lu XC, Zhou SH (2012) Application of uniform design in experiments of WEDM in gas. Adv Mater Res 426:11–14
95. Wiessner M, Macedo FTB, Martendal CP, Kuster F, Wegener K (2018) Fundamental investigation of EDM plasmas, part I: a comparison between electric discharges in gaseous and liquid dielectric media. Procedia CIRP 68:330–335
96. Xiaobing F (2013) Modelling and simulation of crater formation and wire vibration in micro WEDM (doctoral's thesis). National University of Singapore, Singapore
97. Xuyang C, Kai Z, Chunmei W, Zhipeng H, Yiru Z (2015) A study on plasma channel expansion in micro-EDM. Mater Manuf Process 31(4):381–390
98. Yeo SH, Aligiri E, Tan PC, Zarepour H (2009) A new pulse discriminating system for micro-EDM. Mater Manuf Process 24(12): 1297–1305
99. Yu Z, Jun T, Masanori K (2004) Dry electrical discharge machining of cemented carbide. J Mater Process Technol 149(1):353–357
100. Zhang QH, Zhang JH, Ren SF, Deng JX, Ai X (2004) Study on technology of ultrasonic vibration aided electrical discharge machining in gas. J Mater Process Technol 149:640–644
101. Zhang G, Li H, Zhang Z, Ming W, Wang N, Huang Y (2016) Vibration modeling and analysis of wire during the WEDM process. Mach Sci Technol 20(2):173–186
102. Zhou W, Apkarian R, Wang ZL, Joy D (2006) Fundamentals of scanning electron microscopy (SEM). In: Scanning microscopy for nanotechnology. Springer, New York, pp 1–40
103. Zhu Y, Antao DS, Chu KH, Chen S, Hendricks TJ, Zhang T, Wang EN (2016) Surface structure enhanced microchannel flow boiling. J Heat Transf 138:091501
104. Zou R, Yu Z, Yan C, Li J, Qian J (2018) Study of machining characteristics of micro EDM in nitrogen plasma jet. Procedia CIRP 68:559–564